Suplemento de la Revista Mexicana de Física **3** 0308114 (2022) 1–6

Unraveling light nuclei with deeply virtual Compton scattering processes: from models to event generation

S. Fucini and R. Dupré

Université Paris-Saclay, CNRS/IN2P3, IJCLab, 91405 Orsay, France.

Received 25 January 2022; accepted 14 March 2022

In this talk, we present the analysis of a deeply virtual Compton scattering process off ^{4}He. This study is done within the impulse approximation approach including state-of-the-art models for the nucleonic and nuclear ingredients. A glimpse on the comparison between our results and the experimental data coming from Jefferson Lab is also given. The last part of this work is devoted to the description of the new Monte Carlo event generator based on the models presented in the main part of the talk. First results from the simulations performed at the kinematic conditions foreseen at the Electron Ion Collider are discussed demonstrating that there is a wide enough kinematical range to reach the tomography of ^{4}He and understand other possible aspects of the elusive nuclear parton dynamics.

Keywords: Nuclear Compton scattering; nuclear structure; Monte Carlo event generator.

DOI: https://doi.org/10.31349/SuplRevMexFis.3.0308114

1. Introduction

The construction of the Electron Ion Collider (EIC) in the next few decades will shed light on many unanswered questions about the parton structure of nuclei and nucleons [1]. The first evidence of the modification of the parton content of the bound nucleon is dated in the 80's. Then, the European Muon Collaboration (EMC) [2] found with deep inelastic scattering experiments that the structure function of a nucleon in the nuclear medium behaves differently from the one of the free nucleon. This difference cannot be explained only by accounting for the nucleons Fermi motion and conventional calculations do not reproduce precisely this behaviour [3]. To this day, despite the large amount of results collected in this regard, there is not a conclusive explanation for this effect (see, *e.g.*, Ref. [4], for the experimental results obtained at the Jefferson Laboratory (JLab)). Exclusive reactions will play an important role in the investigation of the EMC effect by enriching the information already collected. Thanks to a new generation of experiments at JLab and the forthcoming EIC, new ways to explore the topic have been proposed to achieve a comprehensive explanation of the QCD content of nuclear targets [5, 6]. Such information can be accessed through novel structure functions, in particular the generalized parton distributions (GPDs). These objects are used to achieve a view in three dimensions of the parton content in the coordinate space through the correlation between the space and the momentum degrees of freedom (see, *e.g.*, Refs. [7–9] for an exhaustive report). We can access the GPDs through various exclusive processes; in this talk we will focus on deeply virtual Compton scattering (DVCS), the electroproduction of a single photon. While considering this process off nuclei two channels can occur: the coherent one, where the nucleus remains intact and the tomography of the whole nucleus can ultimately be achieved, and the incoherent one, where, thanks to the breaking up of the nucleus, the structure of the bound nucleon can be retrieved.

In the following, we will focus on the ^{4}He nucleus, whose nuclear effects can realistically be described. Moreover, it is spinless, thus the partonic content of the nucleus can be accounted for by only one GPD; finally, data from JLab exist for both DVCS channels [10,11]. Alongside other existing calculations [12–15], we will propose a workable approach where conventional nuclear physics effects, described in terms of realistic wave functions, are evaluated along the lines proposed in Ref. [16] for the deuteron and in Refs. [17–19] for ^{3}He. In this talk, a review of the main results obtained from the study of the handbag contribution to both DVCS channels is presented. The application of these models in a new Monte Carlo event generator to prepare the future experiments at the EIC will be also presented.

2. DVCS formalism in a nutshell

For a more readable text, in the following the main aspects of the general formalism for both the DVCS channels in the handbag approximation are presented. The impulse approximation (IA) is exploited in our formalism, thus the interaction of the virtual photon with only one quark in one nucleon in ^{4}He can be assumed. Further in the process, after a momentum transfer, the active quark emits a real photon, detected in the final state, before going back into the target itself. Another assumption of the IA is that the actual degrees of freedom are the nucleonic ones and final state interaction (FSI) effects are neglected. As a reference frame, we choose the one where the target is at rest, the initial lepton lies in the *xz* plane and ϕ is the angle between the leptonic and the hadronic planes as well as the azimuthal angle of the outgoing nucleus/proton. The experimental variables used for such a process are: the virtuality of the initial photon $Q^2 = -q_1^2$, the Bjorken variable $x_B = Q^2/2p \cdot q_1$ and the momentum transferred $t = \Delta^2 = (p' - p)^2 = (q_1 - q_2)^2$. In the previous definitions, we denoted as p/p' (q_1/q_2) the initial/final momentum for the nucleus (photon). The other variables appearing in the GPDs definition are x, *i.e.*, the average plus momentum fraction of the struck parton with respect to the total momentum and $\xi = -\Delta^+/(p+p')^{+\ i}$, the difference in plus momentum fraction between the initial and the final states (in principle, GPDs depend also on Q^2 but this dependence will be not discussed for the rest of the paper). While ξ can be related to x_B and thus be measured, x cannot be accessed. Thus, it is instructive to introduce some quantities, the so-called Compton form factors (CFFs), whose expression, for any GPD H, reads

$$\mathcal{H}(\xi,t) = \int_{-1}^{1} dx \frac{H(x,\xi,t)}{x-\xi+i\epsilon} = \mathrm{Pr}\int_{-1}^{1} \frac{H(x,\xi,t)}{x-\xi} - i\pi H(\xi,\xi,t)\,. \quad (1)$$

In the above equation, Pr stands for the Cauchy principal value prescription while the term $(x-\xi+i\epsilon)^{-1}$ comes from the quark propagator between the two photons. Due to the singularities at $x=\xi$, the CFFs $\mathcal{H}(\xi,t)$ are complex quantities that usually are written as

$$\mathcal{H}(\xi,t) = \Re e\mathcal{H}(\xi,t) - i\pi\Im m\mathcal{H}(\xi,t)\,, \quad (2)$$

where, exploiting the symmetry properties of the GPDs, the imaginary and real part are given by

$$\Im m\mathcal{H}(\xi,t) = \sum_q e_q^2 H_q^+(\xi,\xi,t)\,, \quad (3)$$

$$\Re e\mathcal{H}(\xi,t) = \mathrm{Pr}\sum_q e_q^2 \int_0^1 \left(\frac{1}{\xi+x} + \frac{1}{x-\xi}\right) \times H_q^+(x,\xi,t)\,, \quad (4)$$

respectively, in terms of the singlet combination $H_q^{(+)}(x,\xi,t) = H_q(x,\xi,t) - H_q(-x,\xi,t)$ with q the charge of the quarks.

Conversely to GPDs, CFFs can be measured. The key observable is the beam spin asymmetry (BSA) that, for an unpolarized (U) target, can be obtained as

$$A_{LU} = \frac{d\sigma^+ - d\sigma^-}{d\sigma^+ + d\sigma^-}\,, \quad (5)$$

i.e. in terms of the differential cross section for the different beam spin polarization $L = \pm$. A_{LU} is the observable we will focus on for the rest of the paper.

Our realistic plane wave IA studies for the two DVCS channels is detailed in the following sections.

3. Coherent DVCS off ^{4}He

A complete explanation and the relevant plots obtained with our model for the coherent channel can be found in Refs. [20, 21]. Here, the main points of our approach are summarized. The expression for $H_q^{^4He}(x,\xi,\Delta^2)$, *i.e.* the GPD of the quark of flavor q in the ^{4}He nucleus, has been obtained in IA as

$$H_q^{^4He}(x,\xi,\Delta^2) = \sum_N \int_{|x|}^{1} \frac{dz}{z} \int dE \int d\vec{p}\, P_N^{^4He}(\vec{p},\vec{p}+\vec{\Delta},E) \times H_q^N\left(\frac{x}{z},\frac{\xi}{z},\Delta^2\right)\delta\left(z - \frac{\bar{p}^+}{\bar{P}^+}\right), \quad (6)$$

where H_q^N are the GPDs of the bound nucleon N and $P_N^{^4He}(\vec{p},\vec{p}+\vec{\Delta},E)$ is off-diagonal spectral function. It represents the probability amplitude to have a nucleon which leaves the nucleus with momentum $\vec{p}$ and it is reabsorbed after a momentum transfer $\vec{\Delta}$ while the recoiling system has an excitation energy $E^* = E - |E_A| + |E_{A-1}|$, with $|E_A|$ and $|E_{A-1}|$ the nuclear binding energies. In order to achieve a complete evaluation of $P_N^{^4He}$, an exact description of the complete ^{4}He spectrum is needed. Being a challenging theo-

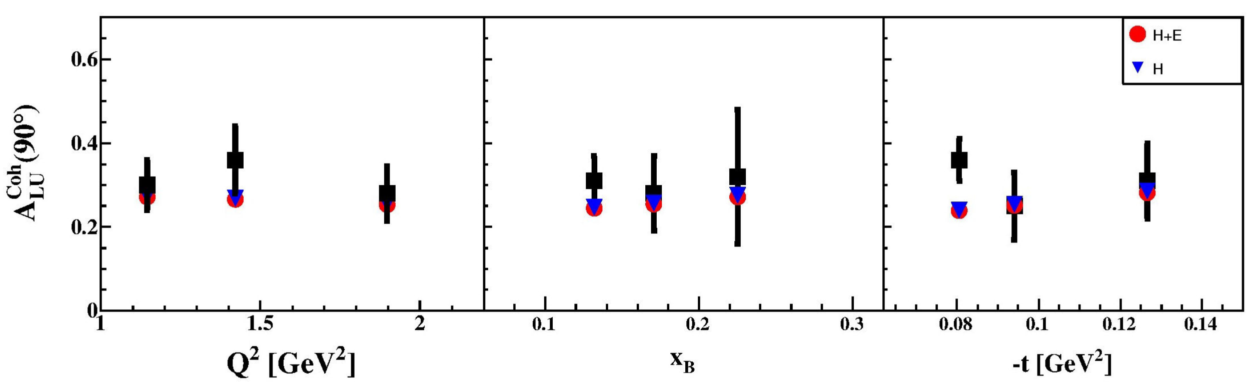

FIGURE 1. (Color online) Azimuthal beam-spin asymmetry for the ^{4}He nucleus, A_{LU}^{Coh} at $\phi = 90^o$: results of our approach (red dots and blue triangles. See Ref. [21] for further discussion) compared with data (black squares) [10].

retical nuclear physics problem, a model for it, based on the diagonal spectral function proposed in Ref. [22], has been used. Our model for the off-diagonal spectral function can be sketched as

$$P_N^{^4He}(\vec{p},\vec{p}+\vec{\Delta},E) = P_0(\vec{p},\vec{p}+\vec{\Delta},E) + P_1(\vec{p},\vec{p}+\vec{\Delta},E) \simeq n_0(\vec{p},\vec{p}+\vec{\Delta})\delta(E) + \sqrt{n_1(|\vec{p}|)n_1(|\vec{p}+\vec{\Delta}|)}\delta(E-\bar{E})\,, \quad (7)$$

where the subscripts 0 and 1 refer to the ground/excited momentum distribution $n(|\vec{p}|)$, respectively, that have been evaluated accounting for Argonne 18 NN interaction [23] and the 3-body forces [24]. In particular, when the recoiling system is in its ground state, the momentum distribution can be realistically evaluated along the lines of Ref. [25] in terms of the exact wave functions of the 3- and 4-body systems, *i.e.*

$$n_0(|\vec{p}|) = |\langle \Phi_3(1,2,3)\chi_4\eta_4 | j_0(|\vec{p}|R_{123,4})\Phi_4(1,2,3,4)\rangle|^2, \quad (8)$$

while the angular dependence has been modeled. As far as the excited part concerns, $n_1(|\vec{p}|)$ has been obtained from the ground and the total momentum distribution so that a realistic momentum dependence is guaranteed. Concerning the removal energy, its dependence is fixed to an average value so that the non diagonal spectral function reduces to the diagonal one (see Ref. [22]). Using this input for the nuclear part and Goloskokov-Kroll (GK) models [26] to evaluate the nucleonic GPDs, the quantities in Eqs. (3) and (4) have been calculated. In this way, also an evaluation of the beam spin asymmetry (5) expressed in terms of the CFFs and kinematical coefficients $\alpha_i(\phi)$ (see Ref. [27] for their expression) as

$$A_{LU}^{Coh}(\phi) = \frac{\alpha_0(\phi)\,\Im m\mathcal{H}(\xi,t)}{\alpha_1(\phi)+\alpha_2(\phi)\,\Re e\mathcal{H}(\xi,t)+\alpha_3(\phi)\Big(\mathcal{H}(\xi,t)\mathcal{H}(\xi,t)^*\Big)}, \quad (9)$$

has been done. A comparison between our predictions and the experimental data [10] for the asymmetry is shown in Fig. 1.

Conclusion: a careful analysis of the coherent DVCS off ^{4}He in terms of basic conventional ingredients turns out to be successful to explain the experimental data at the present accuracy without involving exotic arguments, *e.g.* dynamical off-shellness. Therefore, our model can be actually used as an input in a MC event generator.

4. Incoherent DVCS off ^{4}He

All the details about our IA approach to the handbag diagram of the incoherent channel can be found in Refs. [28, 29]. Our goal is to have a complete evaluation of Eq. (5) and have a comparison with data. The main ingredient we focused on is the cross section for a DVCS process occurring off a bound moving proton embedded in ^{4}He. Accounting for the kinematical off-shellness of the initial proton, one gets the following convolution formula for the cross section

$$\frac{d\sigma^{\pm}_{\text{Incoh}}}{dx_B dQ^2 d\Delta^2 d\phi} = \int_{\text{exp}} dE\, d\vec{p}\, P^{^4He}(\vec{p},E) \times |\mathcal{A}^{\pm}(\vec{p},E,K)|^2 g(\vec{p},E,K)\,, \quad (10)$$

where K is the set of kinematical variables probed in the slice of the phase space exp which selects only the relevant part of the diagonal spectral function $P_N^{^4\text{He}}(\vec{p},E)$ and $g(\vec{p},E,K)$ arises from the integration over the phase space and includes also the flux factor. In the above equation, the squared amplitude includes three terms, *i.e.* $\mathcal{A}^2 = T^2_{DVCS} + T^2_{BH} + \mathcal{I}_{DVCS-BH}$, which have been calculated accounting for the initial motion of the proton and generalize the ones obtained for a proton at rest in Ref. [30].

Since the kinematical region probed at JLab is dominated by the Bethe Heitler (BH) process, considering in Eq. (5) the cross section given in Eq. (10), the BSA can be written as

$$A_{LU}^{Incoh}(K) = \frac{\tilde{\mathcal{I}}_{DVCS-BH}(K)}{\tilde{T}^2_{BH}(K)}\,, \quad (11)$$

where

$$\tilde{\mathcal{A}}(K) = \int dE\, d\vec{p}\, P^{^4He}(\vec{p},E)\, g(\vec{p},E,K)\, \mathcal{A}(\vec{p},E,K)\,, \quad (12)$$

with $\mathcal{A}$, $\tilde{\mathcal{A}} = \mathcal{I}_{DVCS-BH}(K)$, $\tilde{\mathcal{I}}_{DVCS-BH}(\vec{p},E,K)$ and $T^2_{BH}(K)$, $\tilde{T}^2_{BH}(\vec{p},E,K)$. The numerator of Eq. (11), *i.e.* the

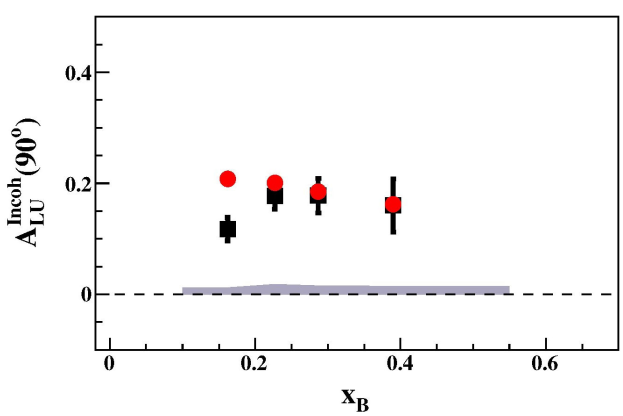

FIGURE 2. (Color online) Azimuthal beam-spin asymmetry for the bound proton on the ^{4}He nucleus for the x_B bin. Results of this approach (red dots) compared with data (black squares) [10]. Shaded areas represent systematic errors.

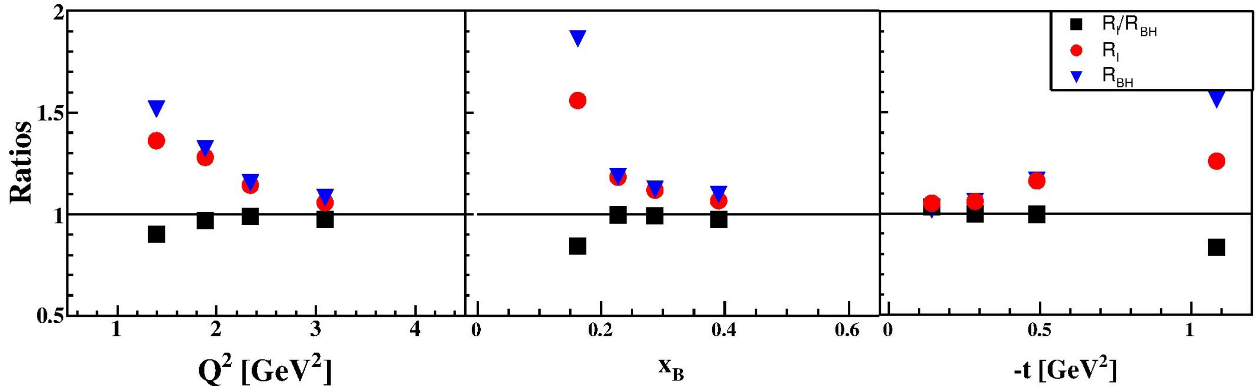

FIGURE 3. The ratios $\tilde{\mathcal{I}}_{DVCS-BH}(K)/I^{free}_{DVCS-BH}$ (red dots), $\tilde{\mathcal{T}}^2_{BH}(K)/T^{2\,free}_{BH}$ (blue triangles), $A^{Incoh}_{LU}(K)/A^{free}_{LU}$ (black squares) at $\phi = 90^o$ and using the GK model for the nucleon GPD. From left to right, the quantity is shown in the experimental Q^2, x_B and t bins, respectively.

DVCS-BH interference amplitude, gives the key partonic information. In our approach, the modification to the inner content of the bound proton is accounted for by the proper definition of ξ' which depends explicitly on the 4-momentum components of the initial proton and thus it is affected by nuclear effects. In the present calculation, we are considering only the dominating contribution given by the $H_q(x, \xi', t)$ GPD, for which use of the GK model has been made [26]. Concerning the diagonal spectral function appearing, for instance, in Eq. (10), we made use of the model presented in Ref. [22]. The results are depicted in Fig. 2; an overall good agreement with experimental data is reached except for the region of lowest Q^2, corresponding to the first x_B bin. As a matter of facts, in this region the impulse approximation can show its limitations and final state interaction effects could come into play. To study the nuclear effects foreseen by our model, we considered the ratio between the asymmetry for an off-shell bound proton and the corresponding quantity for the free proton. This comparison can help us in understanding whether or not the behaviour observed in Ref. [11] is due to a modification of the partonic structure of the proton related to the EMC effect or to other nuclear effects. Our results, see Fig. 4, suggest that what we are finding is due to a different dependence on the 4-momentum components, affected by nuclear effects, of the relevant amplitudes rather than to a modification of the parton structure of the bound proton. More information on this side could be accessed with new tagged measurements with the detection of residual nuclear final states, as planned at JLab [32].

5. Event generation: TOPEG

To evaluate the feasibility of the physics of exclusive reactions on light nuclei at the future EIC, proper MC event generator are needed. In this talk, we present the new MC event generators for the coherent DVCS off ^{4}He, `TOPEG`. The produced cross section exploits our model for the chiral even GPD summarized in Sec. 3. To shorten the time of execution of the simulation, in the present analysis the real part of the CFF has not been included, as we noted that it has a little impact at the considered kinematics. While in Ref. [1] the results for the three energy configurations envisioned at the EIC are presented, here we show the results obtained for 1 million events for a 110 GeV ^{4}He beam and a 18 GeV e^- beam. The kinematical range accessed is: $Q^2 > 4$ GeV^2 and $t_{\min} < |t| < t_{\min} + 0.5$ GeV^2, where

$$t_{\min} = \frac{-Q^2(2(1-x_B)(1-\sqrt{1+\epsilon^2}) + \epsilon^2)}{4x_B(1-x_B) + \epsilon^2}\,, \qquad (13)$$

with $\epsilon = 2Mx_B/Q$. In Fig. 4, the 1-d kinematical distributions of the events as a function of the kinematical variables generated is shown. The generated cross section is clearly dominated by the form factor of the ^{4}He nucleus so that a

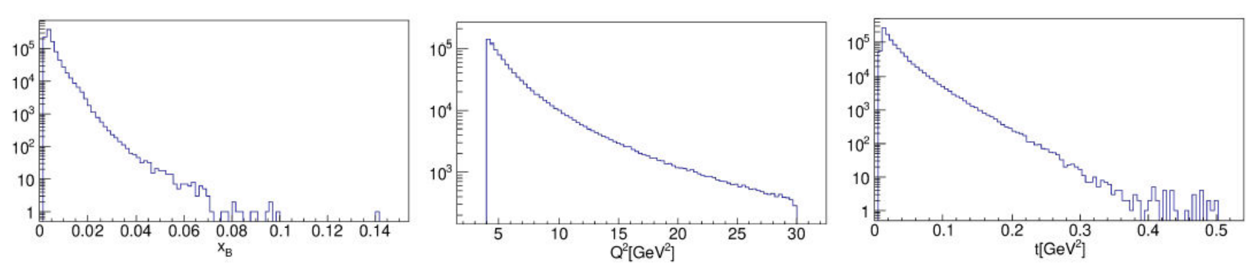

FIGURE 4. One-dimensional distributions of the generated events within `TOPEG` as a function of x_B, Q^2 and $-t$ for the energy configuration 118 GeV (^{4}He) $\times$ 110 GeV (e^-) [1].

strong dependence on t is appreciable in our results. Nevertheless, the value of the cross section is significantly reduced (around 95% or more) when the t acceptance of the helium nuclei in the far forward detectors is accounted for. As a matter of facts, two critical limits to keep in mind in our exploration have been found. On one side, at low $x_B \approx 10^{-4}$, t_{min} becomes very small leading to kinematics almost impossible to access: the reason is that the minimum t is actually set by the detector capabilities (Roman pots). On the other side, we have to deal with a limit on t_{max} that is ultimately set by the luminosity.

As far as the other particles in the final state concerns, 99%+ electrons and photons are in the acceptance of the detector matrix, except for some low angle photons in the backward detector in the highest energy configuration (the one here presented).

Overall, a satisfying enough kinematical range to study the tomography and other features of the nuclear parton dynamics around the critical first diffraction minimum of the ^{4}He electromagnetic form factor has been found. Nevertheless, we identified few key points as critical for these studies which deserve a further investigation currently ongoing.

Acknowledgements

This work has received funding from the European Research Council (ERC) under the European Union's Horizon 2020 research and innovation programme (Grant agreement No. 804480).

---

i. We use the notation $a^{\pm} = \frac{a_0 \pm a_3}{\sqrt{2}}$.

1. R. Abdul Khalek *et al.*, *Science Requirements and Detector Concepts for the Electron-Ion Collider: EIC Yellow Report*, [arXiv:2103.05419[physics.ins-det]]
2. J. J. Aubert *et al.*, [European Muon Collaboration], *The ratio of the nucleon structure functions $F2_n$ for iron and deuterium*, Phys. Lett. **123B** (1983) 275, https://doi.org/10.1016/0370-2693(83)90437-9.
3. A. W. Thomas, *Reflections on the Origin of the EMC Effect*, Int. J. Mod. Phys. E **27** (2019) 1840001, https://doi.org/10.1142/S0218301318400013.
4. J. Seely, A. Daniel, D. Gaskell, J. Arrington, N. Fomin, P. Solvignon, R. Asaturyan, F. Benmokhtar, W. Boeglin and B. Boillat, *et al. New measurements of the EMC effect in very light nuclei*, Phys. Rev. Lett. **103** (2009) 202301, https://doi.org/10.1103/PhysRevLett.103.202301.
5. R. Dupré and S. Scopetta, *3-D Structure and Nuclear Targets*, Eur. Phys. J. A **52** (2016) 159, https://doi.org/10.1140/epja/i2016-16159-1
6. P. R. Norton, *The EMC effect*, Rept. Prog. Phys. **66** (2003) 1253, https://doi.org/10.1088/0034-4885/66/8/201.
7. M. Diehl, *Generalized parton distributions*, Phys. Rept. **388** (2003) 41, https://doi.org/10.1016/j.physrep.2003.08.002.
8. S. Boffi and B. Pasquini, *Generalized parton distributions and the structure of the nucleon*, Riv. Nuovo Cim. **30** (2007) 387, https://doi.org/10.1393/ncr/i2007-10025-7
9. M. Guidal, H. Moutarde and M. Vanderhaeghen, *Generalized Parton Distributions in the valence region from Deeply Virtual Compton Scattering*, Rept. Prog. Phys. **76** (2013) 066022, https://doi.org/10.1088/0034-4885/76/6/066202.
10. M. Hattawy *et al.* [CLAS Collaboration], *First Exclusive Measurement of Deeply Virtual Compton Scattering off ^{4}He: Toward the 3D Tomography of Nuclei*, Phys. Rev. Lett. **119** (2017) 202004, https://doi.org/10.1103/PhysRevLett.119.202004
11. M. Hattawy *et al.* [CLAS Collaboration], *Exploring the Structure of the Bound Proton with Deeply Virtual Compton Scattering*, Phys. Rev. Lett. **123** (2019) 032502, https://doi.org/10.1103/PhysRevLett.123.032502.
12. S. Liuti and S. K. Taneja, *'Microscopic description of deeply virtual Compton scattering off spin-0 nuclei*, Phys. Rev. C **72** (2005) 032201, https://doi.org/10.1103/PhysRevC.72.032201
13. S. Liuti and S. K. Taneja, *Nuclear medium modifications of hadrons from generalized parton distributions*, Phys. Rev. C **72** (2005) 034902, https://doi.org/10.1103/PhysRevC.72.034902
14. V. Guzey and M. Strikman, *DVCS on spinless nuclear targets in impulse approximation*, Phys. Rev. C **68** (2003) 015204, https://doi.org/10.1103/PhysRevC.68.015204
15. V. Guzey, A. W. Thomas and K. Tsushima, *Medium modifications of the bound nucleon GPDs and incoherent DVCS on nuclear targets*, Phys. Lett. B **673** (2009) 9, https://doi.org/10.1016/j.physletb.2009.01.064.
16. E. R. Berger, F. Cano, M. Diehl and B. Pire, *Generalized parton distributions in the deuteron*, Phys. Rev. Lett. **87** (2001) 142302, https://doi.org/10.1103/PhysRevLett.87.142302.
17. S. Scopetta, *Generalized parton distributions of He-3*, Phys. Rev. C **70** (2004) 015205, https://doi.org/10.1103/PhysRevC.70.015205,
18. S. Scopetta, *Conventional nuclear effects on generalized parton distributions of trinucleons*, Phys. Rev. C **79** (2009) 025207, https://doi.org/10.1103/PhysRevC.79.025207.
19. M. Rinaldi and S. Scopetta, *Neutron orbital structure from generalized parton distributions of 3He*, Phys. Rev. C **85** (2012) 062201, https://doi.org/10.1103/PhysRevC.85.062201.

20. S. Fucini, S. Scopetta and M. Viviani, *Coherent deeply virtual Compton scattering off ^4He*, Phys. Rev. C **98** (2018) 015203, https://doi.org/10.1103/PhysRevC.98.015203.
21. S. Fucini, M. Rinaldi and S. Scopetta, *Generalized parton distributions of light nuclei*, Few Body Syst. **62** (2021) 3, https://doi.org/10.1007/s00601-020-01590-0.
22. M. Viviani, A. Kievsky and A. Rinat, *GRS computation of deep inelastic electron scattering on He-4*, Phys. Rev. C **67** (2003) 034003, https://doi.org/10.1103/PhysRevC.67.034003.
23. R. B. Wiringa, V. G. J. Stoks and R. Schiavilla, *An Accurate nucleon-nucleon potential with charge independence breaking*, Phys. Rev. C **51** (1995) 38, https://doi.org/10.1103/PhysRevC.51.38
24. B. S. Pudliner, V. R. Pandharipande, J. Carlson and R. B. Wiringa, *Quantum Monte Carlo calculations of $A \leq 6$ nuclei* Phys. Rev. Lett. **74** (1995) 4396, https://doi.org/10.1103/PhysRevLett.74.4396
25. M. Viviani, A. Kievsky and S. Rosati, *Calculation of the alpha-particle ground state within the hyperspherical harmonic basis*, Phys. Rev. C **71** (2005) 024006, https://doi.org/10.1103/PhysRevC.71.024006.
26. S. V. Goloskokov and P. Kroll, *Transversity in hard exclusive electroproduction of pseudoscalar mesons*, Eur. Phys. J. A **47** (2011) 112, https://doi.org/10.1140/epja/i2011-11112-6.
27. A. V. Belitsky and D. Mueller, *Refined analysis of photon leptoproduction off spinless target*, Phys. Rev. D **79** (2009) 014017, https://doi.org/10.1103/PhysRevD.79.014017
28. S. Fucini, S. Scopetta and M. Viviani, *Catching a glimpse of the parton structure of the bound proton*, Phys. Rev. D **101** (2020) 071501, https://doi.org/10.1103/PhysRevD.101.071501,
29. S. Fucini, S. Scopetta and M. Viviani, *Incoherent deeply virtual Compton scattering off ^4He*, Phys. Rev. C **102** (2020) 065205, https://doi.org/10.1103/PhysRevC.102.065205.
30. A. V. Belitsky, D. Mueller and A. Kirchner, *Theory of deeply virtual Compton scattering on the nucleon*, Nucl. Phys. B **629** (2002) 323, https://doi.org/10.1016/S0550-3213(02)00144-X.
31. C. Ciofi degli Atti and S. Simula, *Realistic model of the nucleon spectral function in few and many nucleon systems*, Phys. Rev. C **53** (1996) 1689, https://doi.org/10.1103/PhysRevC.53.1689.
32. W. Armstrong *et al.*, *Partonic Structure of Light Nuclei*, http://arxiv.org/abs/1708.00888.